Journal of Cluster Science (2026) 37:34
https://doi.org/10.1007/s10876-026-02979-3

ORIGINAL PAPER

Systematic Study of Boron–Nitrogen Molecules: Structures, Stability, and Potential as High-Energy-Density Materials

Maria Fedyaeva[1,2,3] · Sergey Lepeshkin[1] · Artem R. Oganov[3]

Received: 26 April 2025 / Accepted: 4 January 2026

Abstract

Boron-nitrogen nanostructures (molecules and clusters, nanowires, nanotubes; thin films, etc.) have been actively studied in recent years due to their unique physical and chemical properties. These materials hold promise for applications in electronic devices, hydrogen storage, nanodots, and high-strength fibres. In this study we performed a systematic search of B_nN_m molecules in a wide area of compositions ($0 \leq n$, $m \leq 10$) using the evolutionary algorithm USPEX and DFT calculations. We identified a diverse set of structural patterns based on molecular size and B/N ratio. By several criteria (second-order energy differences, fragmentation energies and HOMO-LUMO gaps), we found the most stable ("magic") molecules, which can be formed spontaneously and accumulate in significant concentrations and may serve as building blocks and intermediates for the synthesis and growth of B–N nanoformations. We also revealed that some nitrogen-rich compounds (BN_3, BN_9, B_3N_5, B_4N_6 and B_6N_9) are both "magic" and release significant energy during their decomposition, which indicates their possible application as high-energy-density materials (HEDMs).

Introduction

Over the past decade, a substantial body of theoretical and experimental research has been dedicated to B-N nanostructures including fullerenes[1–4], nanotubes[5–7], nanosheets[5, 8], nanowires[7, 9], and molecules.[10–12] These systems are promising for applications in electronic devices, hydrogen storage, biomedical applications and semiconductor technologies.[13–16] $(BN)_n$ nanostructures are isoelectronic with their carbon analogues and often exhibit higher thermal and oxidative stability, making them attractive for high-temperature applications.[17].

Another promising application of B–N molecules lies in their potential as high-energy-density materials (HEDMs), owing to the substantial energy release upon decomposition. Nitrogen-rich compounds have been extensively investigated in this context, as they liberate large amounts of energy when decomposing with the release of inert N_2 gas.[18] Incorporating other elements can improve their kinetic stability; for example, metal azides such as $Pb(N_3)_2$ are well-known HEDMs.[19]The inclusion of boron can stabilize nitrogen-rich frameworks while preserving the high energy release associated with the formation of N_2. The BN_9 molecule, for instance, has been theoretically predicted and experimentally synthesized[20], but it is stable only at low temperatures (below −35 °C)[21], at higher temperatures undergoing explosive decomposition. The BN_4 molecule has also been suggested as a potential HEDM precursor.[22] However, the synthesis and handling of nitrogen-rich B–N clusters remain challenging due to their extreme sensitivity to thermal, photonic, and mechanical stimuli. These limitations highlight the importance of theoretical exploration in identifying viable HEDM candidates within the B–N system.

Boron-nitrogen molecules B_nN_m are being researched due to their occurrence in the synthesis reactions of mentioned nanoformations. For example, B_2N, BN_2, B_3N, BN_3 and their anions have been obtained by pulsed laser evaporation.[23] However, only molecules with a small number of atoms (e.g., B_3, B_2N, BN_2)[11], or within a narrow range

✉ Maria Fedyaeva
Maria.Fedyaeva@skoltech.ru

[1] Lebedev Physical Institute, Russian Academy of Sciences, 53 Leninskii prosp, Moscow 119991, Russia

[2] Vernadsky Institute of Geochemistry and Analytical Chemistry, Russian Academy of Sciences, Kosygina, 19, Moscow 119991, Russia

[3] Skolkovo Institute of Science and Technology, Bolshoy Boulevard 30, bld. 1, Moscow 121205, Russia

Published online: 07 March 2026

(e.g., B_nN_2 (n=1−6))[24], or stoichiometric molecules (e.g., $(BN)_x$, $2 \leqslant x \leqslant 19$)12 have been studied.

Here we report a systematic detailed ab *initio* investigation of stable boron-nitrogen B_nN_m molecules in a wide range of compositions ($0 \leq n, m \leq 10$). We chose this composition area because it is sufficient to form a systematic picture of the dependence of the structural and energetic properties of clusters on composition, while remaining computationally feasible. We used the global optimization algorithm USPEX and DFT calculations. We studied the geometric and energetic characteristics of B_nN_m molecules, identified the most stable ("magic") ones and estimated energy release associated with the decomposition of each molecule. This allowed us to determine molecules that can serve as potential intermediate states and building blocks in chemical synthesis of more complex B-N structures, as well as potential HEDMs. Thus, in this study we set and pursued two central aims: systematic mapping of B_nN_m structures and identification of promising HEDM candidates among them.

Computational Methodology

To find the optimal structures of boron-nitrogen molecules, we used the evolutionary algorithm USPEX25–28 (see also http://uspex-team.org) coupled with DFT, where each candidate structure was fully relaxed and its total energy was used in the calculation of the fitness. The global search was performed under the explicit constraint that the clusters remain connected, so the geometries are the lowest-energy connected isomers (global minima in this restricted sense). Structure relaxations were performed using the spin-polarised PBE functional29 with the VASP code.30 In these calculations, we used the projector augmented wave method31 and 400 eV plane wave energy cutoff. To model the finite system with a periodic code, the supercell approach was employed, where periodic images of a molecule were separated by a vacuum layer with a thickness of 10 Å. Since we studied isolated molecules, only the Γ-point was used for Brillouin zone sampling. The geometry relaxation was considered converged when the change in total energy between two ionic steps was below 10^{-4} eV. Van der Waals interactions were not explicitly included, as we focused on isolated molecular systems. The 25 lowest-energy isomers from each composition were selected for the final refinement which was done using the B3LYP hybrid functional[32] and 6–311+G(d, p) basis set33 with the Gaussian 16 package. Previous studies showed that results of B3LYP/6-311G* calculations of the geometry and energetics are quite accurate and can be applied to obtain reliable results for B-N molecules.12, 34, 35 During our calculations, spin multiplicities up to 4 were checked. We also calculated vibrational frequencies for each molecule to verify dynamical stability by the absence of imaginary frequencies. ELF analysis shows clear localization of electron density between atoms in the clusters, confirming that they are genuine covalent bonds.

Structure and stability of B_nN_m molecules

We have found the ground-state structures of B_nN_m molecules with the number of atoms n and m from 0 to 10. The obtained structures are either identical to or more energetically favourable to those reported in previous studies: for 41 molecules, we identified the same global minima as previously found; for 5 molecules, we discovered structures with lower energy; and, to the best of our knowledge, structures for 70 compositions were predicted for the first time. A detailed comparison between our results and literature data is given in ESI Section S1. The geometries and energies of all molecules are given in ESI Section S2. The vibrational spectra for each B-N molecule are given in ESI Table S1. The ELF plots for several selected clusters are given in ESI Table S2.

To study the stability of B_nN_m molecules we applied two criteria, which are often used in studies of nanomolecules. (see, e.g. 36, 37). The first one calculates second-order differences over B and N atoms ($\Delta^2{}_B(n, m)$ and $\Delta^2{}_N(n, m)$) and takes the minimal one ($\Delta^2{}_{\min}(n, m)$):

$$\begin{aligned} \Delta^2 B(n,\ m) &= E_{n+1,\ m} + E_{n-1,\ m} - 2E_{n,\ m}, \\ \Delta^2 N(n,\ m) &= E_{n,\ m+1} + E_{n,\ m-1} - 2E_{n,\ m}, \\ \Delta^2 min(n,m) &= min\Delta^2 B(n,m); \Delta^2 N(n,m), \end{aligned} \quad (1)$$

where $E_{n,\ m}$ is the total energy of the molecule containing n boron atoms and m nitrogen atoms. This quantity characterises the resistance against the transfer of one atom between two identical molecules during their collision.Throughout this work, molecules with a positive $\Delta^2{}_{\min}$produce more intense peaks in mass spectra[38–46], which indicates their higher stability and abundance. Figure 1a shows the map of $\Delta^2{}_{\min}(n, m)$ in the composition space, demonstrating the existence of islands and ridges of stability, corresponding to magic molecules. The compositional area of unstable molecules ($\Delta^2{}_{\min}(n, m) < 0$) is marked in blue. In the further analysis of magic molecules we will consider $n \leq 9$ and $m \leq 9$, since for the edge compositions ($n = 10$ or $m = 10$) we cannot calculate both second differences $\Delta^2{}_B$ and $\Delta^2{}_N$.

As shown in Fig. 1a, the most stable B-N molecules are those with a 1:1 stoichiometry - the series $(BN)_x$, with a closed ring-shaped structure and only B-N bonds. B–B and N–N bonds appear naturally in off-stoichiometric compositions: B-rich clusters with B/N atomic ratio > 1 necessarily form B–B linkages, whereas N-rich clusters with B/N < 1 contain N–N bonds . The stability of $(BN)_x$ clusters stems

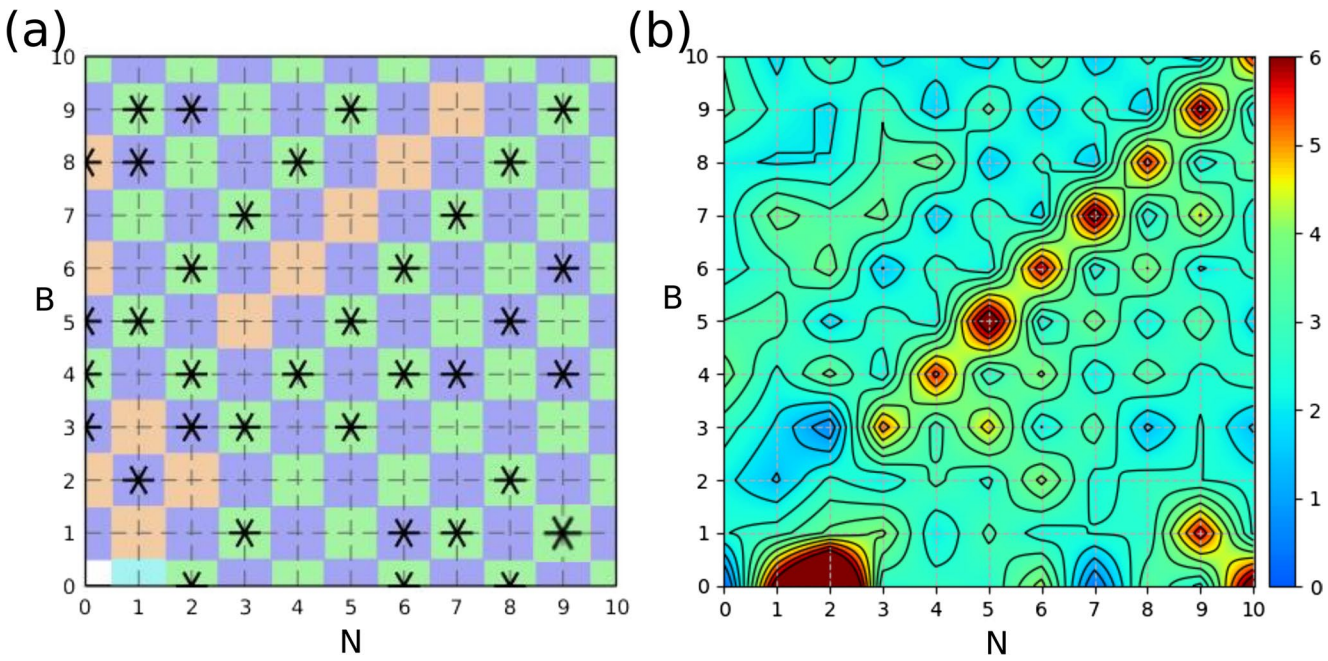

Fig. 1 Interpolated heatmaps showing the stability of B_nN_m molecules using two criteria: (**a**) second-order differences of energy (Δ^2_{min}) and (**b**) fragmentation energy (E_{frag}) into two fragments, both given in eV and shows as a function of n and m.

from the strong covalent bonding between boron and nitrogen atoms and closed-shell electronic structure. However, there is one exception from this rule: the B_2N_2 molecule is unstable due to strained bond angles, yet surprisingly, B_2N with an open-shell electronic structure is a stable one. In general, series of stable compositions looks like ridges for $B/N \geq 1$: B_xN_x ($x=3-9$), $B_{4+x}N_x$ ($x=0-6$), $B_{8+x}N_x$ and $B_{8+x}N_{x+1}$ ($x=0-1$), and separate islands for $B/N<1$: N_2, N_6, N_8, BN_3, BN_6, BN_9, B_2N, B_2N_8, B_3N_5, B_4N_6, B_4N_7, B_4N_9, B_5N_8, B_6N_9. A more detailed discussion of these molecules is given below.

The second criterion is based on the fragmentation energies for all possible fragmentation channels into two fragments $B_nN_m \rightarrow B_kN_l + B_{n-k}N_{m-l}$ with $0 \leq k \leq n$ and $0 \leq l \leq m$:

$$E_{frag}(n,\ m,\ k,\ l) = E(k,\ l) + E(n - k,\ m - l) - E(n,\ m), \quad (2)$$

among which we consider the lowest one:

$$E_{frag}(n,m) = min k,l E frag(n,m,k,l) \quad (3)$$

If $\Delta^2_{min}>0$, then molecules can be formed in significant quantities, and depending on whether the E_{frag} is positive or negative, this molecule will be preserved or decomposed over time. The higher E_{frag}, the more resistant the B_nN_m molecule is to breakup. Heat map of E_{frag} is shown on Fig. 1b. The complete set of fragmentation energies and fission products of all molecules is given in ESI Section S3.

As one can see from Fig. 1b, B_nN_m molecules with $m \leq n$ have large positive values of E_{frag}. In this case, a correlation is observed between Δ^2_{min} and E_{frag}: molecules with a positive Δ^2_{min} usually have higher values of E_{frag} than those with neighbouring compositions. As for nitrogen-rich compounds, molecules with $m=n+1$ (B_nN_{n+1}) have near-zero values of E_{frag}, and for molecules with $m \geq n+2$ E_{frag} is mostly negative (the exceptions are N_2, N_3, BN_3, BN_4, B_2N_4, B_2N_5, B_2N_6, B_3N_5, B_3N_6). The nitrogen-rich molecules with $E_{frag} < 0$ are susceptible to fragmentation, resulting in the emission of an N_2 molecule - a diatomic molecule with a strong triple bond, which is known for its inertness and resistance in various chemical and environmental contexts. The energy release process of decomposition of these molecules will be discussed in more detail below .

Two circumstances make a molecule magical: (1) closed-shell electronic structure (a necessary conditions of which is an even number of electrons), (2) closed-shell atomic structure Indeed, usually molecules with an even total number of electrons are more stable than their neighbors with an odd number. Molecules with odd numbers of electrons also can be magic, especially when they have closed-shell (e.g. symmetric) atomic structure. In the case of B-N molecules, compositions with an even total number of atoms will have an even number of electrons. As a consequence, the stability map of B-N molecules (Fig. 1a) has a nearly checkerboard topology. This expectation holds with many exceptions: not all molecules with an even number of electrons are stable, as indicated by $\Delta^2_{min}<0$, while a number of molecules with an

odd number of electrons are magic: B_2N, B_4N_7, B_4N_9, B_5N_8, B_6N_9, B_8N, B_9N_2 (which often exhibit high symmetry).

We also plotted the map of the optimal spin multiplicities of B_nN_m molecules. Molecules with an even number of electrons have possible multiplicities of 1 or 3 (see Fig. 2a), whereas molecules with an odd number of electrons have only multiplicity of 2 (multiplicity of 4 is energetically favourable only for a single nitrogen atom). From the literature, it is already known that the multiplicity of 3 is characteristic for some pure boron clusters (B_2, B_6, B_8).47 In the current work, we have found that molecules with formula $B_{2+x}N_x$, $x = 0$–7 (with the exception of $x = 2$), BN, B_2N_2 and BN_9 also have a preferable multiplicity of 3 - none of these are magic. For comparison, the energy differences between singlet and triplet states for triplet-favored cases are given in ESI Table S3.

We also calculated the energy gaps between the highest occupied and lowest unoccupied molecular orbitals (HOMO–LUMO gaps, E_g) of the B_nN_m molecules and plotted their map (see Fig. 2b). As electronic polarisation is related to excitation of electrons into unoccupied orbitals, the HOMO-LUMO gap characterises the polarizability of molecules. Large HOMO–LUMO gap indicates closed-shell electronic structure and relatively high chemical inertness, i.e. is indicative of chemical stability. We can see from Figs. 1a and b and 2b, that $E_g(n, m)$ roughly correlates with $\Delta^2_{min}(n, m)$ and $E_{frag}(n, m)$.

Next, a detailed analysis of the geometric features of B-N molecules was conducted. Considering ground-state structures of B_nN_m molecules in the whole compositional area ($n, m = 0-10$), we identified six main structural classes and marked them on the map in the Fig. 3 by different colors: (a) dense nets are marked by deep green color, (b) nets with holes or perforated nets – by red color, (c) ring structures – by purple color, (d) double rings – by light green, (e) rings with rods – by orange color and (f) rods – by blue color. On the right side of Fig. 1 we also show structures of the most stable (magic) molecules of each structural class.

The dense-net structure (Fig. 3a) is characteristic of molecules in which boron predominates and for pure boron clusters. Furthermore, with the addition of nitrogen atoms, the structure becomes less dense and transforms into a perforated net structure (Fig. 3b). With further addition of nitrogen, ring (Fig. 3c) and double-ring structures (Fig. 3d) appear, among which ring $(BN)_x$ compounds have the highest stability. Relatively stable B_8N_4 and B_9N_5 molecules consist of two rings connected through a common segment composed of boron atoms. With further addition of nitrogen, ring structures grow rod-like protrusions, consisting of 2 or 3 atoms of nitrogen (Fig. 3e). Depending on the partial charge of the group, N_2 form species such as pernitrides and diazenides, N_3 - azides. For example, the compound BN_9, which contains three N_3 groups, is referred to as boron triazide. Thus, when the number of boron atoms is low and the number of nitrogen atoms is in great excess, structures with pure nitrogen rod-like fragments are formed (Fig. 3f).

This classification is helpful for the determination of building blocks or intermediate states for the synthesis of more complex B–N formations and nanostructured materials. Dense and perforated nets may fill the space without large voids. This is why they are more appropriate to be building blocks. In addition, perforated nets attract additional interest due to the possibility of their doping (placing extra atoms in the holes) and the resulting creation of new

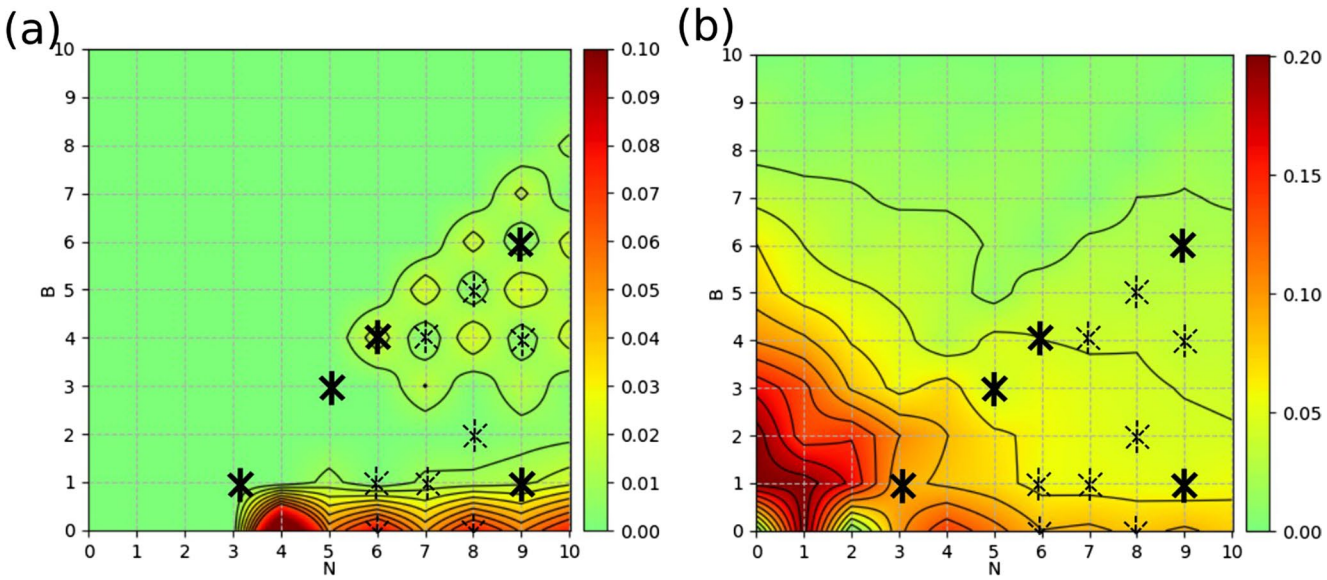

Fig. 2 Electronic characteristics of B_nN_m ($n, m = 0$–10) molecules: (**a**) Multiplicity map (green – $M = 1$, purple – $M = 2$, orange – $M = 3$, blue – $M = 4$), magic molecules ($\Delta^2_{min} > 0$) are marked with asterisks. (**b**) Interpolated heatmap of HOMO-LUMO gaps

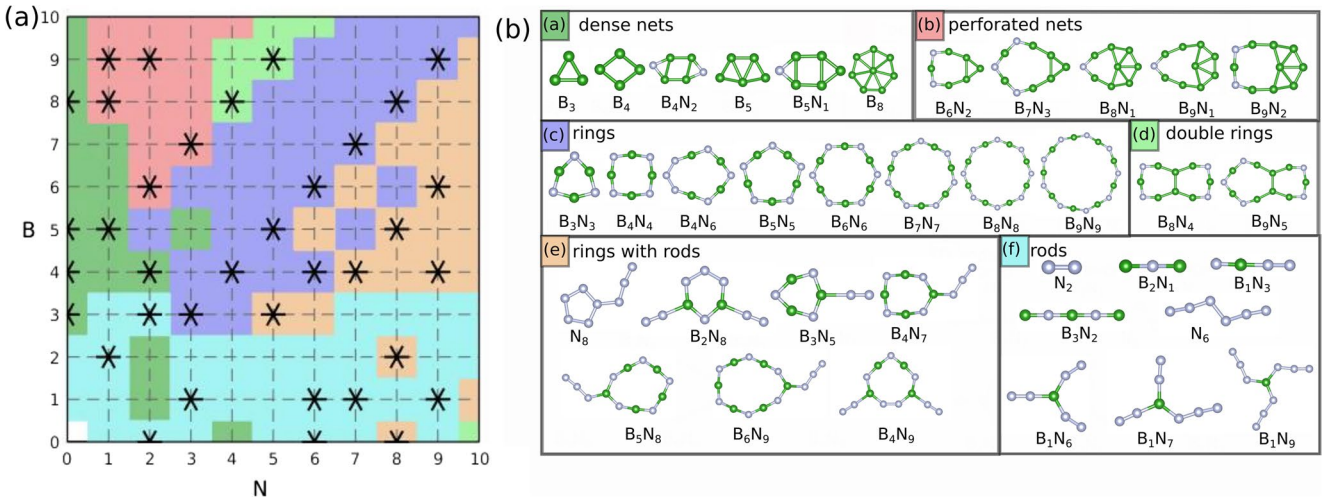

Fig. 3 Chemical diversity of B-N molecules: (**a**) geometric classification, where different structural classes are marked by various colors: **a**) dense nets – deep green color, **b**) perforated nets – red color, **c**) rings – purple color, **d**) double rings – light green, **e**) rings with rods – orange color, **f**) rods – blue color. Magic molecules ($\Delta^2_{min} > 0$) are marked with asterisks.; (**b**) structures of magic molecules of each structural type. Boron (B) is marked by green, nitrogen (N) - by grey

magnetic 2D materials. Rings and double rings have closed structure, which makes them more inert and less prone to react, so they can also act as relatively stable nucleation units for BN sheets or fullerene-like structures. In contrast, rods and rings with rods have at least one terminal atom, which makes them highly reactive – they can significantly modify their structure upon interacting with other particles and may behave as edge or growth units attached to larger BN domains. Both rods and rings, due to their geometry, cannot fill space densely and are interesting only as intermediate states in chemical reactions.

We also inspected the planarity of all obtained molecules (see the planarity classification map ESI Figure S1). We found that the majority of molecules in the studied range of compositions (105 out of 118) are planar, and only 13 molecules are non-planar: B_7, B_9, B_{10}, B_3N_9, B_4N_7, B_5N_{10}, B_6N_9, B_9N_4, $B_{10}N$, $B_{10}N_2$, $B_{10}N_4$, N_5 and N_{10}. B-N non-planar structures tend to twist into a helix (for example, $B_{10}N_4$) or adopt a convex cap-like shape when there is a significant predominance of boron atoms in the structure (for example, $B_{10}N$). Notably, there is no clear relationship between the composition and planarity of the molecules. . For example, the B_4N_6 molecule is planar, while the neighbouring B_4N_7 molecule possesses non-planar structure resembling a cap, and both of them are magic. Planarity in B–N clusters promotes π-delocalization and can enable aromatic stabilization (consistent with Hückel's 4n+2 criterion for planar rings), as exemplified by borazine (B_3N_3). This correlates with higher thermal stability and lower intrinsic reactivity, whereas distorted or nonplanar geometries lose this stabilization and are less practical. Planar B-N rings are therefore more attractive as relatively stable molecular precursors for 2D B-N materials.

B_nN_m molecules as potential HEDMs

This section focuses on exploring the potential use of B_nN_m molecules as HEDMs. Understanding the energies of molecules across the entire compositional range allows us to estimate the energy released during the decomposition of each molecule. We will consider two processes: (1) decomposition of a given molecule into an arbitrary number of fragments, and (2) the decomposition of the corresponding molecular crystal into more stable compounds, where we employ a simplified approach by considering only isolated B_nN_m molecules without including condensed-phase effects or packing density.

(1) First, we calculate the maximum energy that can be obtained from a given molecule by breaking it down into smaller fragments. To accomplish this, we consider decomposition into an arbitrary number (k) of fragments:

$$B_nN_m \rightarrow B_{x1}N_{y1} + B_{x2}N_{y2} + \ldots + B_{xk}N_{yk}, \quad (4)$$

where expressions $x_1+x_2 + \ldots + x_k = n$ and $y_1+y_2 + \ldots + y_k = m$ should be satisfied. The energy release associated with this reaction, normalised by the molar mass of original molecule, is found as:

$$\Delta E_{multi-frag}(n, m, k, x_1, \ldots, x_{k-1}, y_1, \ldots, y_{k-1}) = 1/M(B_nN_m) * (E(n, m) - E(x_1, y_1) - \ldots - E(x_k, y_k)), \quad (5)$$

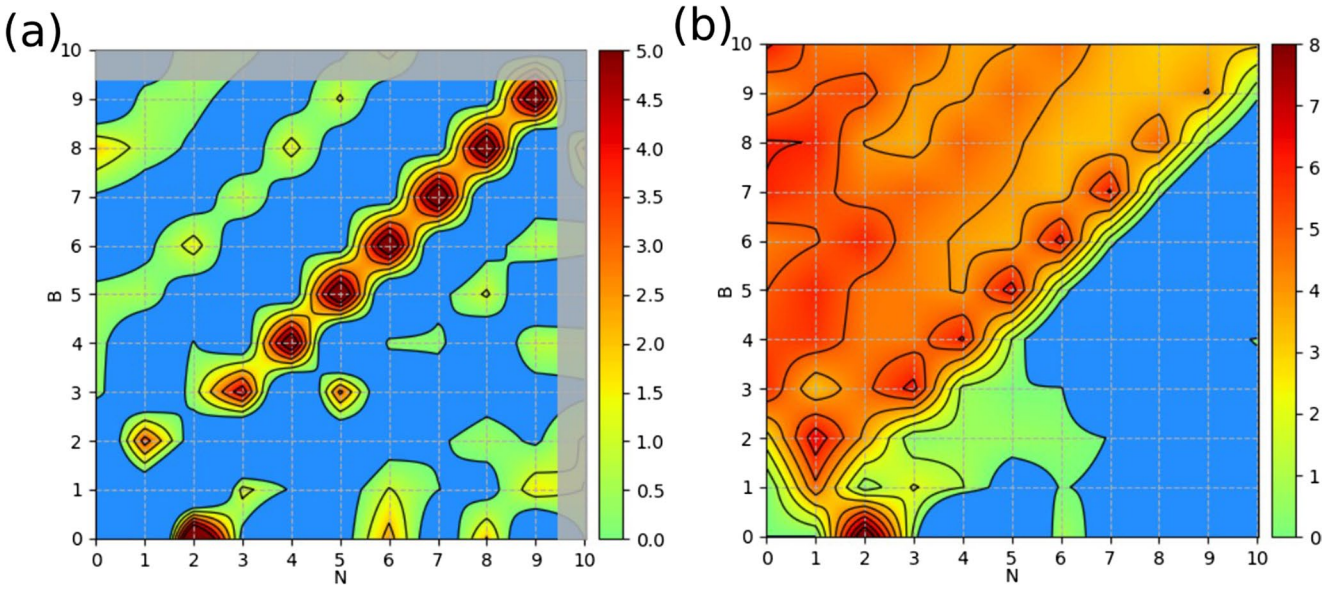

Fig. 4 Interpolated heatmaps showing (**a**) $\Delta E_{\text{multi–frag}}$ - energy release in fragmentation reactions into the most favourable set of smaller molecules and (**b**) $\Delta E_{\text{release}}$ height above the convex hull, where E is the free energy of each molecule in eV as a function of n and m. $\Delta E_{\text{multi–frag}}$ and $\Delta E_{\text{release}}$ are normalised by the molar mass of the original molecule. Magic molecules ($\Delta^2{}_{\text{min}}>0$) which can be chosen as potential HEDMs are marked with asterisks. The most promising ones (that release a substantial amount of energy, $\Delta E_{\text{release}}>1$ MJ/kg) are marked by fat asterisks

where $M(B_nN_m)$ is the molar mass of the B_nN_m molecule and E is the free energy of the molecule. We are looking for the decomposition into such fragments that the released energy reaches a maximum, so it can be found as follows:

$$\begin{aligned}\Delta E_{multi-frag}(n,\ m)\ =\ max_{k,\ x1,\ \ldots,\ xk-1,\ y1,\ \ldots,\ yk-1}\\ \Delta E_{multi-frag}(n,\ m,\ k,\ x_1,\ \ldots,\ xk_{-1},\ y_1,\ \ldots,\ y_{k-1}).\end{aligned} \tag{6}$$

The value of $\Delta E_{\text{multi–frag}}$ essentially shows how much energy can be obtained from a given compound per unit mass. The higher this value, the more promising the molecule is as a high-energy density material (HEDM).

Figure 4a displays the interpolated heat map of $\Delta E_{\text{multi–frag}}(n,\ m)$. The pattern of the $\Delta E_{\text{multi–frag}}$ roughly coincides with the pattern of E_{frag}, taken with the opposite sign: the values of $\Delta E_{\text{multi–frag}}$ are higher for molecules with stoichiometry of N/B$\geq$1. The highest values of $\Delta E_{\text{multi–frag}}$ are reached for pure nitrogen molecules. Magic molecules N_6, N_8, BN_3, BN_6, BN_7, BN_9, B_2N_8, B_3N_5, B_4N_6, B_4N_7, B_4N_9, B_5N_8, B_6N_9 have the potential to be experimentally obtained and have reasonably high $\Delta E_{\text{multi–frag}}$.

(2) Secondly, we aim to estimate the amount of energy released during the decomposition of a molecular crystal composed of the corresponding molecules into the most stable compounds. To this end, we calculate the formation energy for each compound B_nN_m using the formula:

$$\Delta E_{form}\ =\ [E(B_nN_m)\ -\ E(B)*n\ -\ E(N)*m]\ /\ (n\ +\ m), \tag{7}$$

where $E(B_nN_m)$ is the free energy of the B_nN_m compound, and E(B) and E(N) are the energies per atom of the most stable pure boron and pure nitrogen compounds—specifically, the B_{10} cluster and molecular nitrogen (N_2), respectively. We then plot the energy of formation ΔE_{form} as a function of the elemental composition $x=m/(n+m)$ and determine the convex hull of all these points. The points lying on the convex hull correspond to thermodynamically stable phases, and the height above the convex hull (ΔE_{h}) indicates the decomposition energy of a given compound.

In this study, we employ a simplified approach by considering only isolated B_nN_m molecules and neglecting the weak intermolecular van der Waals interactions. This simplification allows us to estimate the energies of formation without performing complex structure predictions of the corresponding molecular crystals. Consequently, for the value of $E(B_nN_m)$ we took the free energy of a single molecule B_nN_m. For pure boron we select B_{10}, the largest boron cluster considered here, which has the lowest energy per atom. For nitrogen, we use the N_2 molecule. The calculated convex hull for all considered B_nN_m molecules is presented in Fig. S1, ESI Figure S2. The compounds lying on the convex hull are B_{10}, $B_{10}N_{10}$, N_2.

Finally, decomposition energy per mass is calculated as follows:

$$\Delta E_{release}\ =\ \Delta E_h * (n\ +m)\ /\ M(B_nN_m). \tag{8}$$

The interpolated heatmap of $\Delta E_{release}$ is shown in Fig. 4b. As example which illustrates that our approximation is reliable and can be effectively applied for estimating the energetic properties of high-energy-density materials we can give well-known HEDM material trinitrotoluene. The height above the convex hull for trinitrotoluene (4.203 MJ/kg) is in close agreement with its experimental decomposition energy (4.190 MJ/kg), which indicates that our approximation is reliable. Based on the data presented in Fig. 4a and b, we observe that the eleven B-N molecules BN_3, BN_6, BN_7, BN_9, B_2N_8, B_3N_5, B_4N_6, B_4N_7, B_4N_9, B_5N_8 and B_6N_9 are promising candidates for HEDMs. These are stable magic molecules (marked by large asterisks in Fig. 4) that release a substantial amount of energy, $\Delta E_{release} > 1$ MJ/kg.

Visible light possesses energies up to 3.3 eV, followed by a UV 'tail' in the spectrum. Molecules with HOMO-LUMO gaps up to about 4 eV will be highly sensitive to light. Molecules with larger values of HOMO-LUMO gaps (≥4 eV) will possess higher photochemical and kinetic stability. This leaves only five promising HEDM molecules: BN_3, BN_9, B_3N_5, B_4N_6, B_6N_9. Interestingly, BN_3 and BN_9 have already been theoretically predicted and subsequently synthesised under low-pressure gas-phase conditions, for example, by the reaction of BCl_3 with HN_3[48, 49]. Main characteristics of the five most promising HEDM molecules among B_nN_m ($0 \le n, m \le 10$) are presented in ESI Table S4. The energy release ($\Delta E_{release}$) for BN_3 molecule is 8.74 MJ/kg, for BN_9 −4.70 MJ/kg, for B_3N_5 −3.91 MJ/kg, for B_4N_6 −4.06 MJ/kg and for B_6N_9 −2.29 MJ/kg, which is ~209%, ~112%, ~93%, ~97% and ~55% of the heat of detonation of trinitrotoluene (4.19 MJ/kg), respectively. Relative to other modern molecular HEDMs — including ICM-101 (oxadiazole)[50], TKX-50 (high-nitrogen salt)51 and neutral N_6[52] (observed only at cryogenic temperature) — our B−N molecules exhibit comparable energy release per mass.

Conclusions

We have predicted the optimal structures of B_nN_m molecules in a wide range of compositions (n, m = 0–10) using the evolutionary algorithm USPEX and DFT calculations. Six principal structural motifs were identified — rods, rings with rods, rings, double rings, dense and perforated nets. Stability was determined using two main criteria: the second-order energy difference ($\Delta^2 E$) and fragmentation energy (E_{frag}), and the results were presented as maps in the compositional space. Based on their geometric and energetic characteristics, we propose a subset of molecules that are likely to serve as intermediates in the synthesis of more complex B–N species. Preferred multiplicities and HOMO-LUMO gaps were also determined for each molecule, providing a basis for further studies of magnetic and optical properties. Our approach to identifying novel high-energy-density materials focuses on species that are both stable (i.e., "magic") and capable of releasing significant energy upon decomposition. For the B–N system, promising candidates are BN_3, BN_9, B_3N_5, B_4N_6 and B_6N_9. We hope these results will motivate future experimental efforts toward the synthesis and application of new B–N molecules.

Supplementary Information The online version contains supplementary material available at https://doi.org/10.1007/s10876-026-02979-3.

Acknowledgements The work was supported by the Project of the State Assignment (Vernadsky Institute of Geochemistry and Analytical Chemistry of Russian Academy of Sciences, Moscow, Russia). The calculations were performed on Oleg and Arkuda supercomputers at Skoltech and at the Joint Supercomputer Center of the Russian Academy of Sciences.

Author Contributions Supervision: A.R.Oganov; Conceptualization: All authors.; Data analysis: M.Fedyaeva and S.Lepeshkin; Methodology: M.Fedyaeva and S.Lepeshkin and A.R.Oganov; Investigation: M.Fedyaeva; Writing – original draft: M.Fedyaeva; Writing – review and editing: All authors.

Data Availability No datasets were generated or analysed during the current study.

Declarations

Competing interests The authors declare no competing interests.

References

1. Golberg, D., Bando, Y., Stéphan, O. & Kurashima, K. Octahedral boron nitride fullerenes formed by electron beam irradiation. Appl. Phys. Lett. 73, 2441–2443 (1998).
2. Seifert, G., Fowler, P. W., Mitchell, D., Porezag, D. & Frauenheim, T. Boron-nitrogen analogues of the fullerenes: electronic and structural properties. Chem. Phys. Lett. 268, 352–358 (1997).
3. Gazzari-Jara, S., Cortés-Arriagada, D., Chigo-Anota, E. & Miranda-Rojas, S. Boron-nitrogen fullerenes as electrocatalysts for nitrogen reduction: A computational study of affinity and reaction mechanism. iScience 28, 112326 (2025).
4. García-Laiton, G., López, F. A. Z., Shakerzadeh, E. & Chigo-Anota, E. Role of homonuclear B–B/N–N bonds in DNA nucleobases adsorption on boron nitride fullerenes: Biosensor and drug transport implications. Comput. Theor. Chem. 1248, 115188 (2025).
5. Golberg, D. et al. Boron nitride nanotubes and nanosheets. ACS Nano 4, 2979–2993 (2010).
6. Golberg, D., Bando, Y., Tang, C. C. & Zhi, C. Y. Boron nitride nanotubes. Adv. Mater. 19, 2413–2432 (2007).
7. Deepak, F. L., Vinod, C. P., Mukhopadhyay, K., Govindaraj, A. & Rao, C. N. R. Boron nitride nanotubes and nanowires. Chem. Phys. Lett. 353, 345–352 (2002).
8. Shtansky, D. V., Firestein, K. L. & Golberg, D. V. Fabrication and application of BN nanoparticles, nanosheets and their nanohybrids. Nanoscale 10, 17477–17493 (2018).

9. Huo, K. F. et al. Synthesis of boron nitride nanowires. Appl. Phys. Lett. 80, 3611–3613 (2002).
10. Sutjianto, A., Pandey, R. & Manuel Recio, J. Structure and stability of BN microclusters: Ab initio calculations for (BN)n (n=2–4). Int. J. Quantum Chem. 52, 199–210 (1994).
11. Martin, J. M. L., François, J. P. & Gijbels, R. A b i n i t i o study of boron, nitrogen, and boron–nitrogen clusters. I. Isomers and thermochemistry of B3, B2N, BN2, and N3. J. Chem. Phys. 90, 6469–6485 (1989).
12. Xu, S.-H. et al. Stability and property of planar (BN)x clusters. Chem. Phys. Lett. 423, 212–214 (2006).
13. Shtansky DV et al (2022) Recent Progress in Fabrication and Application of BN Nanostructures and BN-Based Nanohybrids. Nanomaterials (Basel) 12
14. Nejati, K., Hosseinian, A., Vessally, E., Bekhradnia, A. & Edjlali, L. A comparative DFT study on the interaction of cathinone drug with BN nanotubes, nanocages, and nanosheets. Appl. Surf. Sci. 422, 763–768 (2017).
15. Zhang, L., Cheng, X., Li, X.-H., Chen, J.-H. & Sun, W.-M. A DFT study on the adsorption behavior of antiviral Favipiravir drug on B N (n=12, 16, 20, and 24) nanocages: The size effect. J. Mol. Liq. 360, 119388 (2022).
16. Flores Bautista, M. C., Gómez Conde, J. C., Rodríguez Juárez, A. & Chigo Anota, E. B12N12 structures (pristine, isomer and doped with carbon) for drug delivery: the case of the acetylsalicylic acid. Nano Ex. 6, 015015 (2025).
17. Kostoglou, N., Polychronopoulou, K. & Rebholz, C. Thermal and chemical stability of hexagonal boron nitride (h-BN) nanoplatelets. Vacuum 112, 42–45 (2015).
18. Wang, L. J., Zgierski, M. Z. & Mezey, P. G. Stable structures of nitrogen-rich sulfides: S(N3)m (m=1–4). J. Phys. Chem. A 107, 2080–2084 (2003).
19. Greenwood, N. N. & Earnshaw, A. Chemistry of the Elements. (Elsevier, 2012).
20. Wiberg, E. & Michaud, H. Notizen: Zur Kenntnis eines Bortriazids B(N3)3. Z. Naturforsch. B J. Chem. Sci. 9, 497–499 (1954).
21. Wiberg, E. & Michaud, H. Notizen: Zur Kenntnis eines Bortriazids B(N3)3. *Z. Naturforsch. B* 9, 497–499 (1954).
22. Cheng, L. P., Xu, Y. Q., Wang, G. L. & He, H. H. Theoretical study of BN4: potential precursors of high energy density materials (HEDMs). J Mol Model 18, 1927–1934 (2012).
23. Martin, J. M. L., El-Yazal, J., François, J.-P. & Gijbels, R. The structure and energetics of B3N2, B2N3, and BN4. Mol. Phys. 85, 527–537 (1995).
24. Cui, W., Wang, C., Shao, J. & Zhu, X. Geometry, stability, and isomerization of B n N2 (n=1–6) isomers. Int. J. Quantum Chem. 113, 2251–2260 (2013).
25. Lepeshkin, S. V., Baturin, V. S., Uspenskii, Y. A. & Oganov, A. R. Method for Simultaneous Prediction of Atomic Structure and Stability of Nanoclusters in a Wide Area of Compositions. J. Phys. Chem. Lett. 10, 102–106 (2019).
26. Lyakhov, A. O., Oganov, A. R., Stokes, H. T. & Zhu, Q. New developments in evolutionary structure prediction algorithm USPEX. Comput. Phys. Commun. 184, 1172–1182 (2013).
27. Oganov, A. R., Lyakhov, A. O. & Valle, M. How evolutionary crystal structure prediction works–and why. Acc. Chem. Res. 44, 227–237 (2011).
28. Oganov, A. R. & Glass, C. W. Crystal structure prediction using ab initio evolutionary techniques: principles and applications. J. Chem. Phys. 124, 244704 (2006).
29. Perdew, J. P., Burke, K. & Ernzerhof, M. Generalized gradient approximation made simple. Phys. Rev. Lett. 77, 3865–3868 (1996).
30. Kresse, G. & Furthmüller, J. Efficient iterative schemes for ab initio total-energy calculations using a plane-wave basis set. Phys. Rev. B Condens. Matter 54, 11169–11186 (1996).
31. Blöchl, P. E. Projector augmented-wave method. Phys. Rev. B Condens. Matter 50, 17953–17979 (1994).
32. Lee, C., Yang, W. & Parr, R. G. Development of the Colle–Salvetti correlation-energy formula into a functional of the electron density. Phys. Rev. B 37, 785–789 (1988).
33. Stephens, P. J., Devlin, F. J., Chabalowski, C. F. & Frisch, M. J. Ab initio calculation of vibrational absorption and circular dichroism spectra using density functional force fields. J. Phys. Chem. 98, 11623–11627 (1994).
34. Atiş, M., Özdoğan, C. & Güvenç, Z. B. Structure and energetic of Bn (n=2–12) clusters: Electronic structure calculations. Int. J. Quantum Chem. 107, 729–744 (2007).
35. Nirmala, V. & Kolandaivel, P. Molecular interaction of H2 and H2O molecules with the boron nitride (BN)n=3–5 clusters: A theoretical study. Theochem 758, 9–15 (2006).
36. Arab, A. & Habibzadeh, M. Theoretical study of geometry, stability and properties of Al and AlSi nanoclusters. J. Nanostructure Chem. 6, 111–119 (2016).
37. Hashemi, Z., Rafiezadeh, S., Hafizi, R., Hashemifar, S. J. & Akbarzadeh, H. First-principles study of MoS2 and MoSe2 nanoclusters in the framework of evolutionary algorithm and density functional theory. Chem. Phys. Lett. 698, 41–50 (2018).
38. Li, X.-P. et al. Structures and stabilities of Pb(n) (n<or=20) clusters. J. Phys. Chem. A 113, 6217–6221 (2009).
39. Wang, C., Cui, W., Shao, J., Zhu, X. & Lu, X. Exploration on stability, aromaticity, and potential energy surface of planar BnC2 (n=3–8). Comput. Theor. Chem. 1006, 19–30 (2013).
40. He, C., Shao, J., Shi, R. & Zhu, X. On the geometries, stabilities, and potential energy surfaces of planar C4B2 and C2B4. Comput. Theor. Chem. 967, 59–66 (2011).
41. Shao, J. et al. Exploration of structures and stability of planar CnB3 (n=1–8). Theochem 961, 17–28 (2010).
42. McAnoy, A. M., Bowie, J. H. & Blanksby, S. J. A theoretical study of C4B isomers. The interconversion of CCBCC and CCCCB via cyclic C4B. J. Phys. Chem. A 107, 10149–10153 (2003).
43. Wang, C., Cui, W., Shao, J., Zhu, X. & Lu, X. Exploration on the structure, stability, and isomerization of planar C n B5 (n=1–7) clusters. Int. J. Quantum Chem. 113, 2514–2522 (2013).
44. Boustani, I. Systematic ab initio investigation of bare boron clusters:mDetermination of the geometryand electronic structures ofBn(n=2–14). Phys. Rev. B Condens. Matter 55, 16426–16438 (1997).
45. Truong, B. T., Grant, D. J., Nguyen, M. T. & Dixon, D. A. Thermochemistry and electronic structure of small boron clusters (B(n), n=5–13) and their anions. J. Phys. Chem. A 114, 994–1007 (2010).
46. Wang, Y., Zhou, Y., Zhang, Y. & Buhro, W. E. Magic-size II-VI nanoclusters as synthons for flat colloidal nanocrystals. Inorg. Chem. 54, 1165–1177 (2015).
47. Lepeshkin, S. V., Baturin, V. S., Naumova, A. S. & Oganov, A. R. 'Magic' Molecules and a New Look at Chemical Diversity of Hydrocarbons. J. Phys. Chem. Lett. 13, 7600–7606 (2022).
48. Hobbs, Keith, and Robert D. Coombe. "A New Approach to the Dissociation of BN9 for BN Thin Films." (1999).
49. Mulinax, R. L., Okin, G. S. & Coombe, R. D. Gas phase synthesis, structure, and dissociation of boron triazide. *J. Phys. Chem.* 99, 6294–6300 (1995).
50. Zhu, S. *et al.* Chemical insights into the initial thermolysis reactions of [2,2'-bi(1,3,4-oxadiazole)]-5,5'-dinitramide (ICM-101) from quantum chemical modeling. *Chem. Phys.* **595**, 112684 (2025).

51. Liu, D. *et al.* An overview on synthesis, explosion, catalysis, modification, and application of dihydroxylammonium 5,5′-bistetrazole-1,1′-diolate (TKX-50). *Chem. Mater.* **36**, 3496–3535 (2024).
52. Qian, W., Mardyukov, A. & Schreiner, P. R. Hexanitrogen (N6): A Synthetic Leap Towards Neutral Nitrogen Allotropes. ChemRxiv (2024) doi:https://doi.org/10.26434/chemrxiv-2024-90vvx.